Elucidating the pathogenesis underlying bicuspid aortic valve disease using new disease models

Pol, V. van de

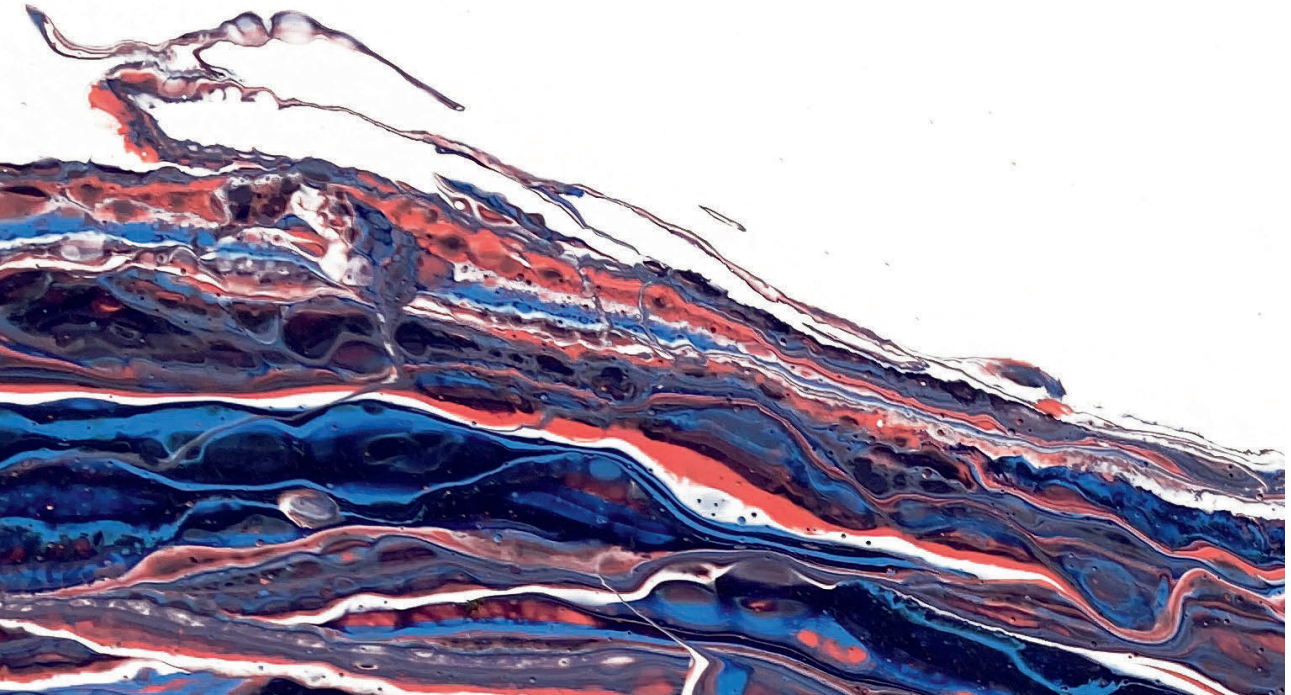

Chapter 5

Inflammation induces endothelial-to-mesenchymal transition and promotes vascular calcification through down regulation of BMPR2

Gonzalo Sánchez-Duffhues[1], Amaya García de Vinuesa[1], Vera van de Pol[1], Marlieke E. Geerts[2], Margreet R. de Vries[2], Stef G. T. Janson[1], Hans van Dam[1], Jan Lindeman[2], Marie-José Goumans[1], Peter ten Dijke[1]

[1]Department of Cell and Chemical Biology, Oncode Institute. Leiden University Medical Center, Leiden, The Netherlands.
[2]Department of Vascular Surgery. Leiden University Medical Center, Leiden, The Netherlands.

Published: Journal of Pathology, 2019 | 3: p. 333

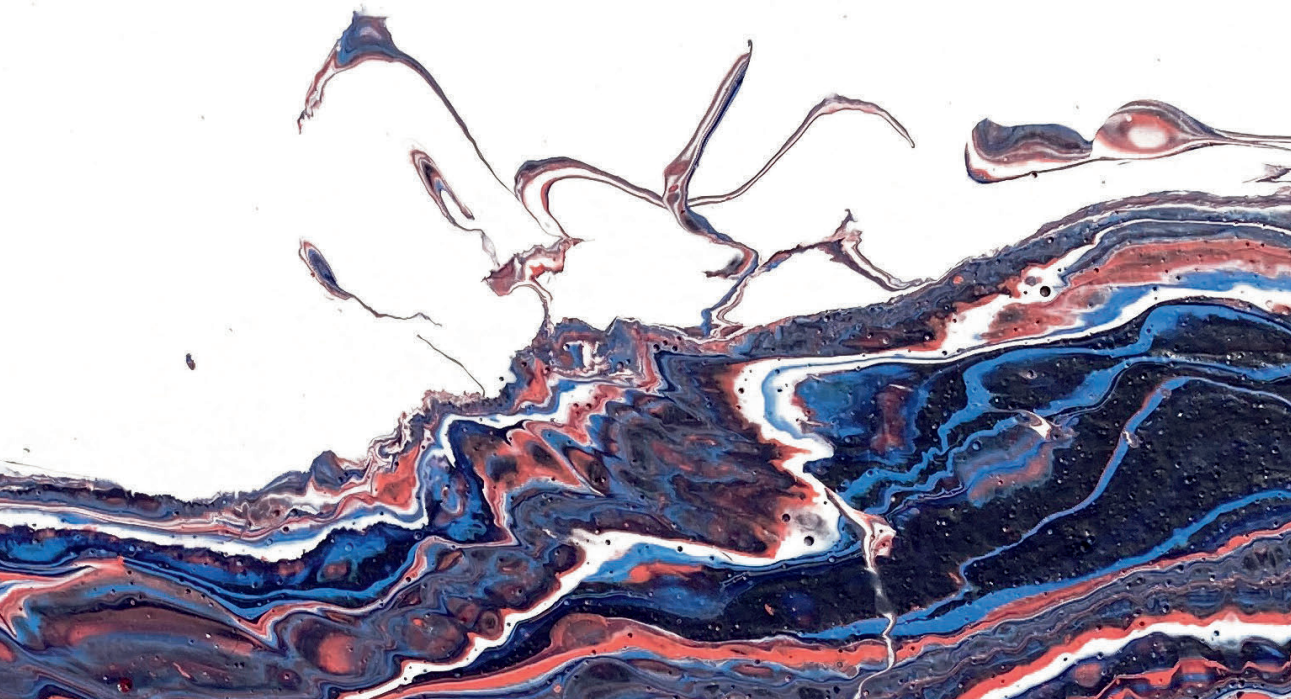

Abstract

Endothelial-to-mesenchymal transition (EndMT) has been unveiled as a common cause for a multitude of human pathologies, including cancer and cardiovascular disease. Vascular calcification is a risk factor for ischemic vascular disorders and slowing calcification may reduce mortality in affected patients. The absence of early biomarkers hampers the identification of patients at risk. EndMT and vascular calcification are induced upon cooperation between distinct stimuli, including inflammatory cytokines and Transforming growth factor (TGF)-β family growth factors. However, how these signaling pathways interplay to promote cell differentiation, and eventually, vascular calcification is not well understood. Using in vitro and ex vivo analysis in animal models and patient-derived tissues, we have identified that the proinflammatory cytokines tumor necrosis factor (TNF)-α and interleukin (IL)-1β induce EndMT in human primary aortic endothelial cells, thereby sensitizing them for BMP-9-induced osteogenic differentiation. Down regulation of the BMP type II receptor BMPR2 is key event in this process. Rather than compromising BMP canonical signal transduction, loss of BMPR2 results in decreased JNK signaling in ECs, thus enhancing BMP-9-induced mineralization. Altogether, our results point at the BMPR-JNK signaling axis as a key pathway regulating inflammation-induced EndMT and contributing to calcification.

Introduction

Vascular calcification is a prevalent feature in cardiovascular diseases associated with elevated risk of mortality. The underlying cellular and molecular mechanisms involved have been an area of intense study in recent decades. Mineralization of blood vessels occurs through a coordinated crosstalk between different cell types and cytokines, but ultimately relies on osteoblast lineage cells for the actual synthesis and mineralization of the calcified matrix [1]. We and others have shown that endothelial cells (ECs) can function as an additional source of osteogenic progenitors in vascular calcification [2-4]. ECs can undergo a process known as Endothelial-to-Mesenchymal transition (EndMT), which involves loss of endothelial features and acquisition of a fibroblast-like phenotype, eventually leading to cells with osteogenic potential. EndMT is modulated by different extracellular growth factors (i.e., Transforming growth factor (TGF)-β family ligands, inflammatory cytokines, fibroblast growth factors), and conditions (i.e., mechanical stress, hypoxia) (reviewed in [5]). Noteworthy, during the onset and progression of calcified plaques in aorta, both inflammatory cytokines, such as tumor necrosis factor (TNF)-α and interleukin (IL)-1β [6], and TGF-β family ligands, including the bone morphogenetic proteins (BMPs) [7,8], coincide in the affected area. Whereas BMP-2 and BMP-4 mainly have a paracrine function, BMP-9 and BMP-6 are found in systemic circulation [9]. BMP-9 has been shown to regulate vascular homeostasis, by regulating proliferation [10], angiogenesis [11], permeability [12] and monocyte recruitment [13]. Interestingly, BMP-9 has been shown capable of inducing heterotopic ossification when expressed ectopically using adenovirus [14]. Noteworthy, administration of BMP antagonists prevents experimental atherosclerosis in preclinical animal models [15,16], highlighting the relevance of this pathway in the context of atherosclerosis.

TGF-β signaling is initiated with the oligomerization of receptor complexes at the cell membrane upon ligand binding. BMPs signal via complexes consisting of a type I receptor named Activin receptor-like kinase (ALK)1/2/3/6; and one of three possible type-II receptors: BMPR2, activin type II receptor A and B (ACVR2A, ACVR2B) [17]. Receptor activation induces the phosphorylation of SMAD1/5/8, which form heteromeric complexes with SMAD4 and translocate into the nucleus to regulate the expression of genes. In osteogenic cells, BMPs induce the transcription of genes related with osteoblast differentiation and activation [18]. In addition to this so-called canonical SMAD signaling pathway, TGF-β family ligands modulate the activity of different mitogen activated protein (MAP) kinases, including ERK (Extracellular signal-Regulated Kinases), p38 kinases and JNK (c-JUN N-terminal protein Kinase) in a cell specific and context-dependent fashion [19,20]. Furthermore, how BMP signaling is fine-tuned

by inflammation in EndMT-derived cells and cells with osteogenic potential is yet to be determined. Whereas it has been suggested that inflammatory stimuli inhibit BMP signaling and osteoblast differentiation and activation [21,22], others have shown that inflammation is needed for osteogenesis [23,24].

In this manuscript, we investigate the interplay between inflammation and BMP signaling in ECs. We found that TNF-α and IL-1β induce EndMT in primary ECs, which become prone to undergo osteogenic differentiation in response to BMP-9. We identified BMPR2 down regulation as a key event in this process, which leads to decreased JNK activation, thereby enhancing BMP-9 induced mineralization. Finally, we supported our findings in a preclinical animal model of atherogenesis, as well as patient derived tissues from atherosclerotic donors. Our results provide a better understanding on the molecular mechanisms underlying EndMT and vascular calcification and may have broad implications for other human inflammatory pathologies involving BMP signaling.

Materials and methods

Cell culture and reagents

Human aortic endothelial cells (HAoECs, CC-2535, Batch number 0000316662), pulmonary aortic endothelial cells (PAEC, CC-2530) and coronary microvascular endothelial cells (cMVECs, CC-7030) were purchased from Lonza. Human skin microvascular endothelial cells (HMECs) were described elsewhere [25]. All cells were cultured in complete EBM-2 medium (Lonza) on 1% w/v gelatin coated wells. Endothelial colony forming cells (ECFCs) were isolated as previously described [26] and cultured in complete EBM-2 medium. All experiments were performed with cells grown to near confluency between passage 6-8. 2H-11 cells are derived from endothelial cells isolated from lymph nodes of adult C3H/HeJ mice transformed using SV40 and have been reported previously [27,28]. These cells were grown on 1% w/v gelatin coated dishes (Merck) in DMEM medium (Invitrogen) supplemented with 4.5 g/L D-glucose (Invitrogen), 110 mg/L sodium pyruvate (Invitrogen), non-essential amino acids (Invitrogen), 10% (v/v) heat inactivated Fetal Bovine Serum (Sigma-Aldrich Chemie), 0.5% (v/v) antibiotic/antimyotic solution (Invitrogen) and 2mM L- glutamine (Invitrogen).

EndMT assays

HAoECs were seeded confluently in 12 wells plates (for qPCR analysis), or Lab-Tek II chamber slides (for immunofluorescent labeling) in EBM2 complete medium containing 2% FBS. Next day, the cells were stimulated with the indicated ligands for 24 hours in EBM2 complete medium containing 10% FBS.

Subsequently, expression of endothelial and mesenchymal specific markers was analyzed by quantitative RT-PCR or immunofluorescent labeling.

Osteoblast differentiation assays

To study osteoblast differentiation, formation of calcium and phosphate deposits was analyzed by Alizarin Red Solution staining. The cells were seeded in 48 wells plates confluently. For HAoECs, the cells were pretreated with TNF-α (10 ng/mL) or TGF-β_3 (5 ng/mL) for 4 days in EBM2 containing 10% of FBS. Next, the medium was replaced by osteogenic medium (DMEM containing 10% FBS, 10^{-8} mol/L dexamethasone, 0.2 mmol/L ascorbic acid and 10 mmol/L β-glycerol-phosphate) in the presence of BMP-9 (10 ng/mL) for 14 days. For 2H-11 cells, they were incubated with the aforementioned osteogenic medium containing both TNF-α (10 ng/mL) and BMP-9 (10 ng/mL) for 14 days. The medium was refreshed every 4 days. Afterwards cells were washed twice with PBS and fixed with 3.7% formaldehyde for 5 minutes. Next, cells were washed twice with distilled water and measurement of calcium deposition was performed by Alizarin Red Staining (ARS), as previously described [29]. Precipitates originated from 3 independent ARS assays were dissolved using 10% cetylpyridinium chloride and absorbance was measured at 570 nm. Representative pictures were obtained using a Leica DMIL LED microscope with 10 times magnification.

Quantitative RT-PCR

Total RNA extraction was performed using NucleoSpin RNA II (MACHEREY-NAGEL). 500 ng of RNA were retro-transcribed using RevertAid First Strand cDNA Synthesis Kits (Fermentas), and real-time reverse transcription-PCR experiments were performed using SYBR Green (Bio-Rad) and a Bio-Rad machine. The primers used in this study are indicated as online supplemental information. *Gapdh* was used for normalization.

Immunofluorescent labeling on cultured cells

HAoECs grown on coverslips were fixed with 4% formaldehyde for 30 minutes at room temperature, washed with glycine for 5 minutes, permeabilized with 0.2% Triton X-100 and blocked in PSB containing 5% BSA for one hour. Next, the cells were incubated overnight at 4C in blocking solution containing primary antibody with gentle shaking. Next day, the cells were washed 5 times in washing buffer (PBS containing 0.05% Tween-20 and 1% BSA) and incubated with secondary antibody (Alexa Fluor FITC goat anti-mouse IgG, Alexa-Fluor 555 anti-rabbit IgG (Invitrogen, 1:200) or Phalloidin-488 (1:100) in PBS with 0.5% BSA for one hour. Finally, the cells were washed 5 times in washing buffer and

mounted in Prolong Gold containing DAPI (Invitrogen). After careful drying, the preparations were imaged in a Leica SP5 confocal scanning laser microscope. A representative picture from each staining is shown (n = 3). The antibodies used are described in online supplemental information.

Western Blotting

Cells were seeded into 12-well plates and cultured till they reached confluence. Next, cells were stimulated as indicated and then washed with cold PBS. Cells were lysed in 2x sample buffer as previously described [30]. A more complete protocol description and the antibodies used can be found in online supplemental information.

Lentiviral production and transduction

Lentiviral vectors were produced in HEK293T cells as described before [29]. Lentiviral vectors expressing specific shRNAs were obtained from Sigma (MISSION® shRNA). The shRNA constructs used in this study can be found at Online Supplement. Lentiviral vectors to over-express mMKP-1 have been described before [31].

Vein graft procedure

Vein grafts were performed as reported elsewhere [32]. A detailed explanation of the method can be found in online supplemental information.

Immunostaining on tissues

In short, immuno-fluorescent and -histochemical stainings on human and murine aortic tissues were performed as previously described [3]. Detailed protocols and list of antibodies used can be found in online supplemental information. 4 μm human aortic sections were prepared from each donor and classified according to the revised classification of the American Heart Association (AHA), as proposed by Virmani et al., by two independent observers with no knowledge of the donor characteristics [33,34]. Sample collection and handling was performed in accordance with the guidelines of the Medical and Ethical Committee in Leiden, Netherlands and the code of conduct of the Dutch Federation of Biomedical Scientific Societies.

Transfections, luciferase assays and DNA constructs

For luciferase reporter assays, cells were seeded in 24-well plates and transfected with DharmaFECT Duo (Thermo Fisher Scientific), following the recommendations of the manufacturer. 48 hours after transfection the cells were harvested

and lysed. Luciferase activity was measured using the luciferase reporter assay system from Promega) by a Perkin Elmer luminometer Victor^3 1420. Each transfection mixture was equalized with empty vector when necessary and every experiment was performed in triplicate. The BRE-Luc reporter has been reported elsewhere [35]. The expression vector encoding the constitutively active fusion protein MKK7-JNK3 and its characterization has been previously described [36].

Iodination and ligand affinity labeling of cell surface receptors.

Iodination of BMP9 was performed according to the chloramine T method and cells were subsequently affinity labelled with the radioactive ligand as described before [37]. Cell lysates were immunoprecipitated with specific antibodies against ALK1, ALK2, BMPR2 and ACVR2A. The generation and characterization of these antibodies have been previously published [38][39][40]. Image quantification was performed by densitometry using Image J analysis.

Statistical analysis

Student's *t*-test was used for statistical analysis and * $P < 0.05$; ** $P < 0.01$; *** $P < 0.001$ was considered significant. All experiments were performed at least three independent times. The results are shown as the mean ± SD of the mean of three independent experiments. Reproducible results were obtained, and representative data are shown in the figures.

Results

TNF-α and IL-1β induce EndMT in HAoECs, thereby enhancing BMP-induced-mineralization in HAoECs

In order to determine the mechanisms by which ECs contribute to the generation of atherosclerotic plaques, we used primary human coronary aortic endothelial cells (HAoECs) stimulated with the indicated pro-inflammatory cytokines and members of the TGF-β superfamily of growth factors. After 24 hours, TNF-α and IL-1β induced a decrease in the expression of the endothelial markers *CDH5* (encoding for VE-CADHERIN) and *Pecam-1*, and an up-regulation of the mesenchymal genes *CDH2* (encoding for N-CADHERIN) and *Fibronectin* (Figure 1A). Accordingly, these two cytokines significantly up-regulated the expression of *SNAI1* and *TWIST1* (Figure S1). This correlated with the loss of the typical endothelial cobblestone-like phenotype, as seen by cytoskeletal staining with Phalloidin, and the down regulation of VE-CADHERIN, PECAM-1 and TIE2, and increase in N-CADHERIN, αSMA and VIMENTIN (Figure 1B). Furthermore, pretreatment with TNF-α sensitized HAoECs to become osteoblast-like

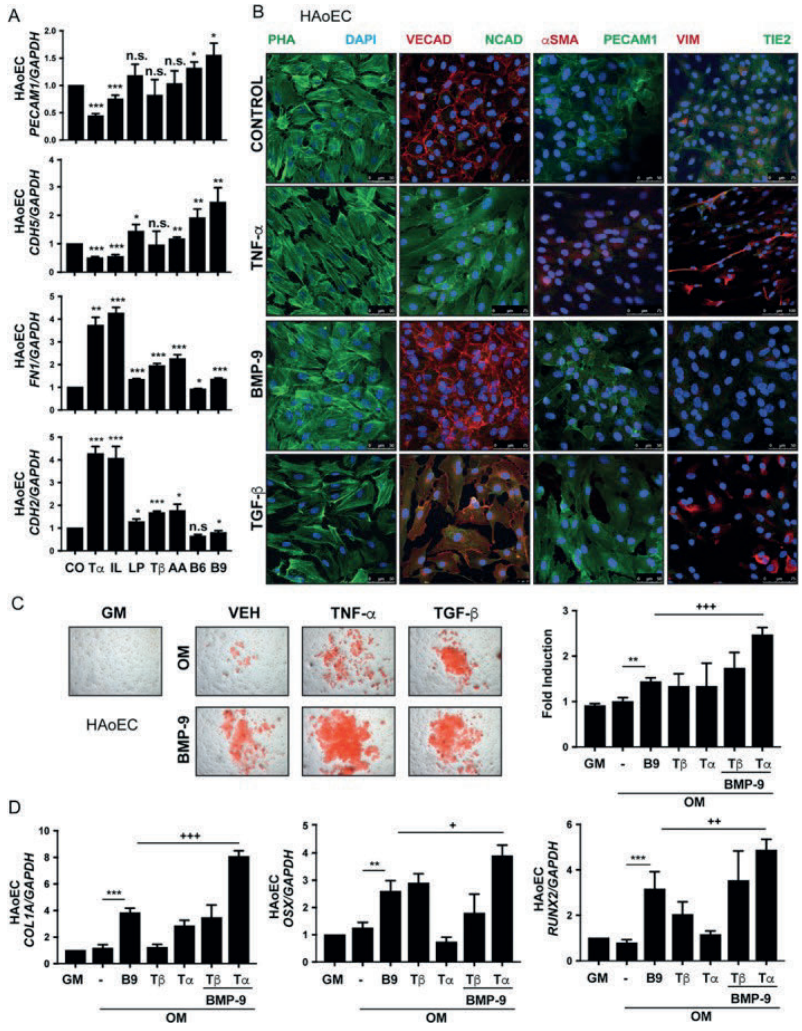

Figure 1. The pro-inflammatory cytokine TNF-α induces EndMT in HAoECs, priming them for BMP-9-induced osteogenic differentiation. A. Gene expression of analysis of the genes Cdh5 (encoding for VE-CADHERIN), Pecam1, Fibronectin and Cdh2 (encoding for N-CADHERIN) in HAoECs stimulated for 24 hours with the indicated cytokines and growth factors. CO: control; Tα: TNF-α (10 ng/mL); IL: IL-1β (10 ng/mL); LP: LPS (10 ng/mL); Tβ: TGF-β_3 (5 ng/mL); AA: activin A (50 ng/mL); B6: BMP-6 (50 ng/mL); B9: BMP-9 (10 ng/mL). B. Immunofluorescent staining on HAoECs stimulated with TNF-α, BMP-9 or TGF-β_3 as previously mentioned. PHA (Phalloidin), VECAD (VE-CADHERIN), NCAD (N-CADHERIN), αSMA, PECAM-1, VIM (Vimentin) and TIE2. C. Alizarin Red Solution staining and corresponding quantification on HAoECs incubated with BMP-9 for 21 days under osteogenic conditions, after induction of EndMT with TNF-α or TGF-β. Quantification is shown at the right side. GM: Growth medium; OM: osteogenic medium. D. qPCR analysis of the osteogenic genes Collagen-1-alpha-1 (Col1a1), Osterix (Osx) and Runx2 in HAoECs subjected to osteogenic differentiation.

cells in response to BMP-9, more potently than TGF-β, as shown by Alizarin Red Solution (ARS) staining (Figure 1C), and the enhanced expression of the osteogenic genes *Collagen 1 alpha 1* (Col1a), *Runx2* and *Osterix* (Osx) (Figure 1D). We found that TNF-α alone induced the expression of *BMP7* and the combination of BMP-9 and TNF-α induced the up-regulation of the osteogenic *BMP2*, and *BMP4* (Figure S2). These results show that the pro-inflammatory cytokine TNF-α induces EndMT in HAoECs and that EndMT derived cells exhibit an enhanced osteogenic response to BMP-9.

BMPR2 down-regulation is necessary and sufficient for TNF-α to induce EndMT in HAoECs

BMP-9 signaling in ECs is mediated by two possible type I receptors ALK1 and or ALK2, and three type II receptors, BMPR2, ACVR2A and ACVR2B [41]. We investigated whether the expression of the BMP type II receptors is modified by stimuli inducing EndMT, thereby enhancing the osteogenic response of BMP-9. As shown in Figure 2A, the two potent EndMT inducers TNF-α and IL-1β triggered a clear down regulation of BMPR2, whereas ACVR2A and ACVR2B were not affected. This effect correlated with a decreased mRNA expression of *BMPR2* (Figure S3), and was not exclusive of HAoECs, as endothelial colony forming cells (ECFCs) and, to a lesser extent, human skin microvascular ECs (HMECs), displayed a similar response (Figure S4). Noteworthy, incubation with higher concentrations of TNF-α led to a reduced expression of all three BMP type II receptors (Figure S5). We next investigated whether BMPR2 down regulation is necessary for TNF-α to induce EndMT in HAoECs, using knockdown and overexpression experiments (Figure 2B). Knock down of *BMPR2* in HAoECs using two different shRNA constructs resulted in reduced *CDH5* and *Pecam-1*, and increased *CDH2* and *Fibronectin* gene expression and loss of endothelial morphology. In contrast, ectopic overexpression of a full length BMPR2 construct (BMPR2 FL) in HAoECs using lentiviral particles prior to TNF-α stimulation prevented TNF-α-induced EndMT, as shown by gene expression analysis (Figure 2C) and immunofluorescent labeling (Figure 2D,E). Altogether our results show that down-regulation of BMPR2 is required for TNF-α to induce EndMT in HAoECs, and BMPR2 over-expression can partially prevent EndMT.

BMPR2 is down-regulated in ApoE3Leiden mice in response to high fat diet We next aimed to validate our findings *in vivo* using an animal model of atherosclerosis. The contribution of EndMT to vascular calcification and atherosclerosis has been recently investigated in different animal models, including $LDLR^{-/-}$, ApoE deficient or Ins^{Akita} mice [4,42,43]. The ApoE3Leiden mice constitute a valuable model of diet-induced atherosclerosis with a human-like lipoprotein

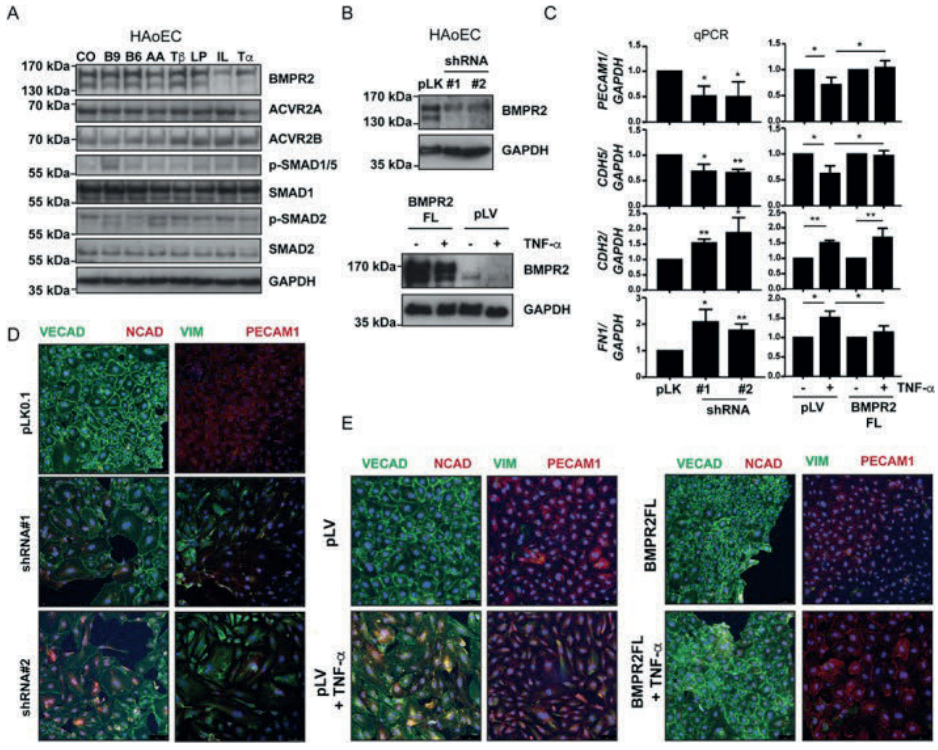

Figure 2. TNF-α-induced down regulation of BMPR2 is necessary for HAoECs to undergo EndMT. A. Western blot in HAoECs where EndMT has been induced for 24 hours as shown in Figure 1A. B. Western blot in HAoECs transduced with a control (pLK) lentivirus or two shRNA constructs (#1 and #2) against BMPR2 (upper panel) or with lentivirus encoding a full-length version of BMPR2 (BMPR2 FL) and treated with TNF-α for 24 hours (lower panel). C-E. EndMT analysis by qPCR (C) and Immunofluorescent staining (Ve-Cadherin, N-Cadherin, Vimentin, Pecam-1) (D and E) in HAoECs knocked-down for BMPR2 or over-expressing BMPR2 FL.

profile, when fed with a high fat diet [30,39]. Furthermore, this model is currently considered one the animal models of native atherosclerosis closest to the human pathology. Although some aspects of this model have been characterized already (e.g., a strong inflammatory infiltrate potentiates plaque's development), the contribution of EndMT to plaque formation is not known yet. Therefore, we performed immunofluorescent co-stainings for Pecam-1 and αSMA on sections from control animals (7 days normal diet vein grafts) and high hypercholesterolemic diet (high fat diet, HFD)-induced atherosclerosis animals (after 7, 14 and 28 days). As previously reported [32], the luminal endothelial layer of the aorta of HFD fed mice down-regulated Pecam-1 expression after 7 days, in contrast to control animals (Figure 3A, low magnification). This was accompanied by evident neointimal thickening. Interestingly, we observed Pecam-1 and αSMA

double positive cells migrating from the luminal layer into the neointima area (Figure 3A, high magnification). Such phenomenon was visible from day 7-28 in HFD fed animals, with a progressive increase in the expression of αSMA in the neointima. Consistent with our *in vitro* findings, BMPR2 expression was markedly reduced in the aorta at the onset of atherosclerosis, as early as 7 days of administration of HFD (Figure 3B).

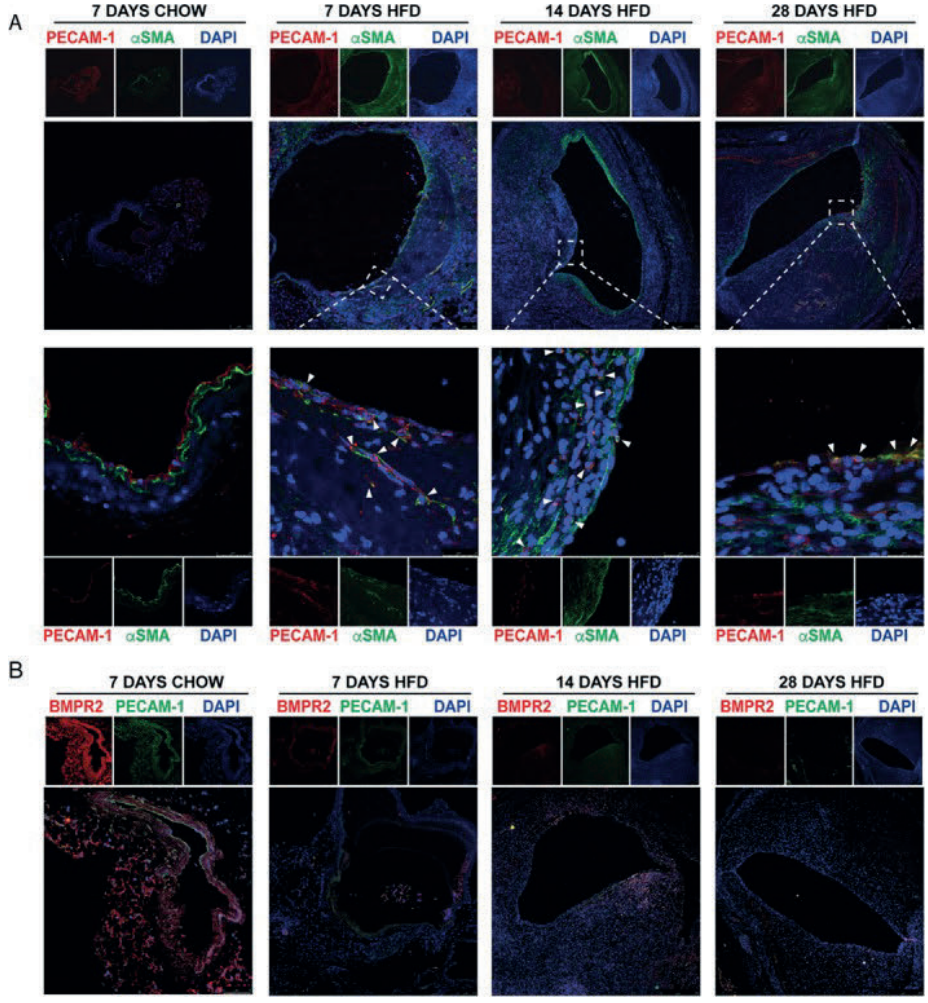

Figure 3. BMPR2 is downregulated in the aorta of ApoE3Leiden mice developing atherosclerotic disease. Aortic sections from ApoE3Leiden mice fed with a normal (Chow) or high fat diet (HFD) for 7, 14 or 28 days and stained for PECAM-1 and αSMA (A) or BMPR2 and PECAM-1 (B). A representative picture per condition is shown. White arrows point at PECAM-1/αSMA double positive cells, suggestive of EndMT.

Down regulation of BMPR2 does not compromise BMP-induced canonical SMAD1/5 signaling

In order to investigate the mechanisms by which loss of BMPR2 induced by TNF-α enhanced the osteogenic differentiation of ECs in response to BMP-9, we characterized an easy-to-culture EC line, the 2H-11 murine ECs. First, we demonstrated that, BMP-2, BMP-6, BMP-7 and BMP-9 effectively induce cell calcification in 2H-11 cells (Figure S6A), which can be blocked by coincubation with a BMP type I receptor kinase inhibitor (Figure S6B). Moreover, similar to primary HAoECs, knock-down of *BMPR2* (and not *ACVR2A* or *ACVR2B*) enhanced the osteogenic differentiation of 2H-11 cells induced by BMP-9 (Figure S7 and S8). On the contrary, stable overexpression of *BMPR2* FL partially prevented the osteogenic effect of BMP-9 (Figure S9). Since one of the main determinants of osteogenic differentiation is the induction of BMP canonical SMAD1/5 signal transduction, we first analyzed whether this was affected by TNF-α. Although TNF-α pretreatment of 2H-11 cells resulted in a dose-dependent increase in osteogenic differentiation of BMP-9-induced 2H-11 cells (Figure 4A), the canonical BMP-9-induced transcriptional response (as measured using the BRE-LUC reporter construct, Figure 4B) was not increased by TNF-α. Using a previously reported protocol for Iodination and ligand affinity labeling of cell surface receptors, we studied the high affinity receptors for BMP-9 in 2H-11 cells. As Figure 4C shows, while BMP-9 mainly forms a receptor complex including BMPR2 in control conditions, upon knock-down of *BMPR2*, BMP-9 recruits ACVR2A in a receptor signaling complex, together with ALK1/2 (Figure S10). To investigate whether this affects the canonical signaling response to BMP-9 in 2H-11 cells, we performed western blotting in stably knocked-down 2H-11 cells for *BMPR2*, *ACVR2A* or *ACVR2B*. As expected, single knock-down of any of the type II receptors failed to compromise BMP-9-induced p-SMAD1/5 response. Interestingly, pre-treatment with TNF-α blocked p-SMAD1/5 activation exclusively in cells knocked-down for ACVR2A (Figure 4D). These results suggest that loss of BMPR2 induced by TNF-α, leads to an enhanced recruitment of ACVR2A in the signaling receptor complex, in order to balance downstream canonical signaling in ECs.

Down regulation of BMPR2 decreases JNK pathway activation to fine tune EC mineralization

Since the enhanced osteogenic response to BMP-9 of ECs lacking BMPR2 was not related to BMP-9 canonical signaling, we next tested the effect of different chemical inhibitors of non-canonical signaling on BMP-9-induced osteogenic differentiation. We used SP600125 to inhibit c-JUN N-terminal kinase (JNK), UO120

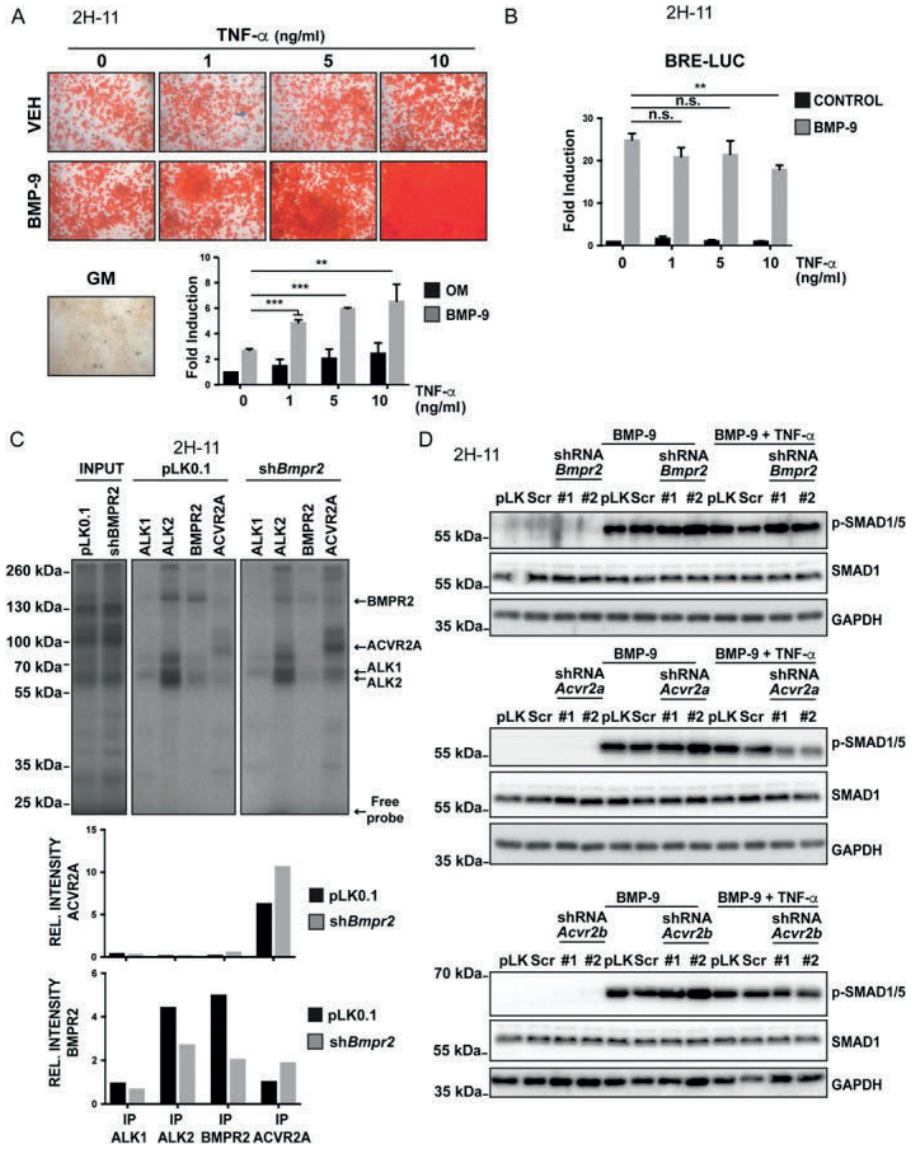

Figure 4. TNF-α-induced loss of BMPR2 does not compromise BMP-9 canonical signaling in ECs. A. Alizarin Red staining and quantification (lower figure) in 2H-11 cells incubated with BMP-9 (10 ng/ml) and increasing concentrations of TNF-α. GM: growth medium. Statistical significant difference with respect to control or BMP-9/TNF-α-treated cells (**, *** or non significant). B. BMP-9-induced canonical transcriptional response in 2H-11 cells stimulated with BMP-9 (10 ng/ml) upon pre-incubation with TNF-α. Fold induction of untreated control cells is shown. C. Ligand–receptor interaction assay in 2H-11 cells stably knocked down for BMPR2 or a control vector (pLK0.1). Quantification is shown below. D. Western blot of p-SMAD1/5 and total SMAD1 in 2H-11 cells stably knocked down for *Bmpr2, Acvr2A* or *Acvr2B* and treated with BMP-9 (10 ng/ml) and TNF-α (10 ng/ml).

against Extracellular signal related kinase (ERK), SB203580 for p38 kinase and PDTC (Ammonium pyrrolidinedithiocarbamate) to block Nuclear factor kappa B (NF-κB) signaling. We found that among all inhibitors used, only SP600125 enhanced the osteogenic differentiation of 2H-11 cells (Figure 5A). We confirmed this using a mutant version of the phosphatase MKP-1 (mMKP-1) [31]. 2H-11 cells transduced with mMKP-1 showed decreased activation of p-c-JUN, a downstream target of JNK, in response to BMP-9 (Figure S11). Next, we investigated the activation of p-c-JUN in 2H-11 cells stably knocked-down for BMPR2 or the other type II receptors. As Figure 5B shows, down regulation of *BMPR2,* and not ACVR2A or ACVR2B, by two different shRNA constructs decreased p-c-JUN in response to BMP-9. Furthermore, chemical inhibition of JNK in shBMPR2 2H-11 cells failed to enhance the calcifying effect of BMP-9, unlike control (pLK0.1), shACVR2A and shACVR2B stable cells (Figure 5C). This might suggest that BMPR2 functionally interacts with JNK in order to activate JNK signaling, as it has been previously suggested [44,45]. Accordingly, endogenous JNK was detected in GST pull down experiments performed with GST-BMPR2 (Figure S12). Finally, In order to determine the contribution of JNK signaling to the osteogenic differentiation of 2H-11 cells, we restored JNK signaling in cells with stable knock-down of *BMPR2* by over-expressing the MKK7-JNK3 fusion protein, which induces constitutive activation of JNK [36]. Ectopic over expression of MKK7-JNK3 increased the levels of phospho-c-JUN (Figure S13). Interestingly, this correlated with a partial inhibition of BMP-9-induced mineralization (Figure 5D). Taken together these data confirm that down-regulation of JNK activity in ECs favors their osteogenic differentiation in response to BMPs.

ECs forming the *vasa vasora* in advanced human atherosclerosis exhibit reduced BMPR2 expression and JNK activation

A unique characteristic of human atherosclerosis consists in the progressive ingrowth of micro capillaries from the adventitia towards the intima in the aorta. We have previously shown that ECs lining such capillaries (known as *vasa vasora*) increase the expression of the transcription factor Slug in early stages on atherosclerosis [3], suggesting that these cells may undergo EndMT and thereby contribute to a population of cells with osteogenic potential. To further extend these studies, we performed immunofluorescent labeling on sections of the human aorta corresponding to different stages of the atherosclerosis spectrum [34]. We observed an accumulation of αSMA positive cells and loss of luminal PECAM-1 in microcapillaries from sections corresponding to Fibrotic Calcified Plaque

(Advanced) (Figure 6A). Noteworthy, we found double positive PECAM-1 αSMA cells around the luminal endothelium, which is suggestive of EndMT.

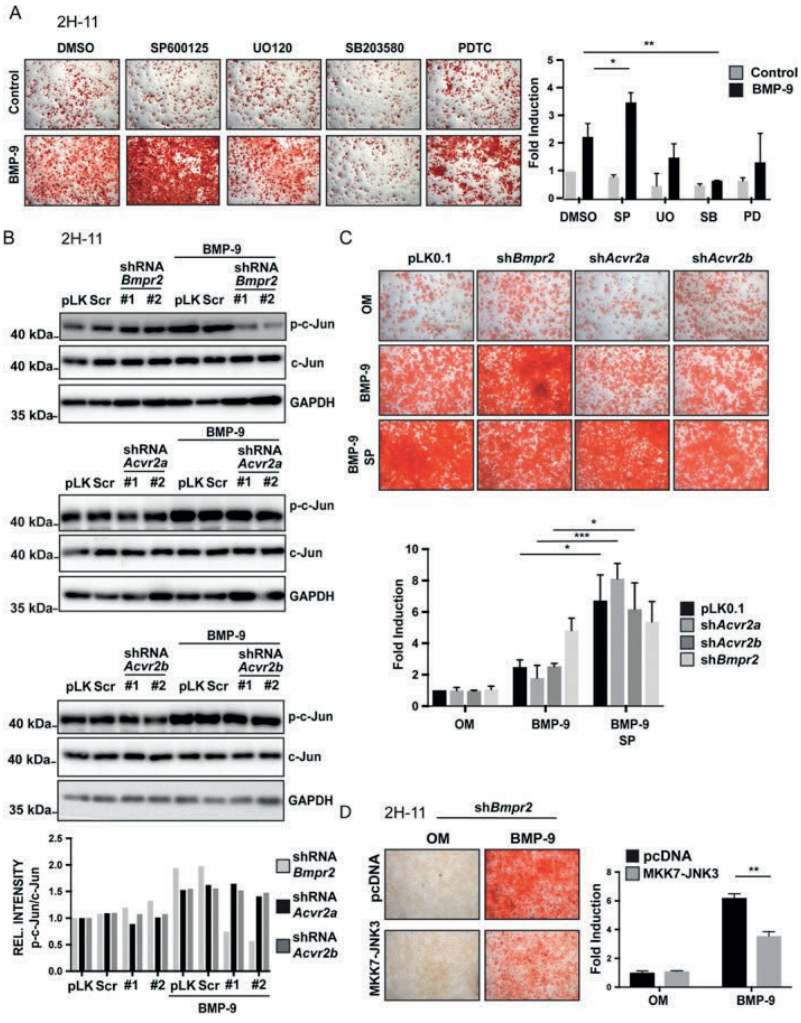

Figure 5. Loss of BMPR2 decreases c-JUN activation, thereby enhancing BMP-9-induced osteogenic differentiation of ECs. A. Alizarin Red Solution (ARS) staining and quantification on 2H-11 cells co-treated for 14 days with BMP-9 (10 ng/mL) and chemical inhibitors targeting the JNK (SP600125, 5 μmol/L), ERK (UO120, 10 μmol/L), p38 (SB203580, 10 μmol/L) and NF-κB (PDTC, 50 μmol/L) signaling pathways, incubated under osteogenic conditions. Fold induction of DMSO treated control cells is shown. B. Western blot of p-c-JUN and total c-JUN in 2H-11 cells stably knocked-down for *BMPR2*, *ACVR2A* or *ACVR2B* and stimulated with BMP-9 (10 ng/mL) for 45 mins. Quantification is shown below. C. ARS staining and quantification on 2H-11 cells stably knocked-down for BMPR2 (shRNA #1), ACVR2A (shRNA #1) or ACVR2B (shRNA #1) and stimulated for 14 days with BMP-9 (10 ng/mL) or BMP-9 and SP600125 (5 μmol/L) in osteogenic conditions. OM: Osteogenic medium. D. ARS staining and quantification in 2H-11 cells stably knocked-down for *BMPR2* and transfected with MKK7-JNK3 or an empty vector (pcDNA3), incubated with BMP-9 (10 ng/mL) under osteogenic conditions. Fold induction of pcDNA-transfected untreated cells is shown. OM: Osteogenic medium.

Furthermore, whereas BMPR2 was very potently expressed in ECs from capillaries of Normal and Early fibroatheroma (Early) sections (Figure 6B), ECs in Advanced lesions were very poorly stained for BMPR2 and PECAM-1. Finally, we analyzed the nuclear expression of p-SMAD1/5 and p-c-JUN in vasa vasorum ECs (Figure 6C,D). As Figure 6E shows, ECs expression of p-SMAD1/5 significantly augmented in Early and remained elevated in Advanced lesions. On the contrary, p-c-JUN expression peaked in Early stages, and dramatically dropped in Advanced lesions, in agree with the loss of BMPR2 expression. Altogether, these results support the mechanisms we have identified *in vitro*, and propose BMPR2 as a novel biomarker and druggable target for human atherosclerosis.

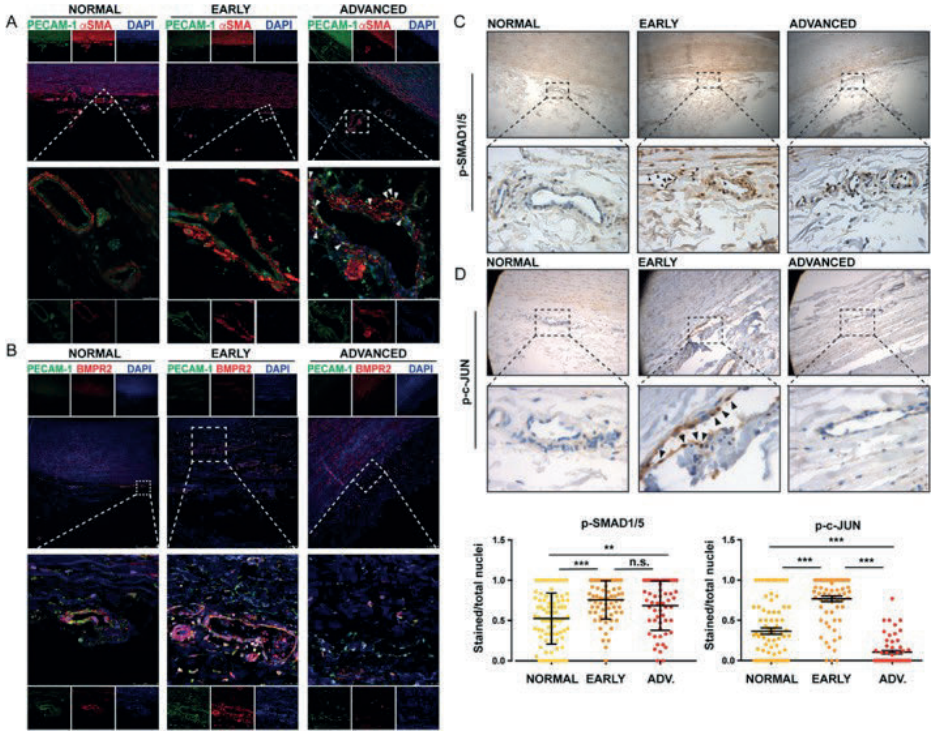

Figure 6. BMPR2 is downregulated in ECs of advanced lesions of human atherosclerosis. Immunofluorescent staining on aortic sections of control, Early Fibroatheroma (Early) or Fibrotic calcified plaque (FCP) donors. A representative picture per condition is shown. Zoomed images focus on microcapillaries in intimal and medial regions underneath the fibrotic core. A. Staining for PECAM-1 (green), αSMA (red) and DAPI (blue). White arrows point at PECAM-1 αSMA double positive cells. B. Staining for PECAM1 (green), BMPR2 (red) and DAPI (blue). Immunohistochemical staining for p-SMAD1/5 (C) or p-c-JUN (D) on the aforementioned sections. Black arrows point at positively stained cells. Low magnification (10X) and zoomed images (40X) are shown. E. Quantification of (C) and (D), based on number of p-SMAD1/5 or p-c-JUN positive ECs nuclei in one vessel/total nuclei in such vessel. A minimum of 55 vessels from 3 independent donors were considered per condition.

Discussion

The identification of patients at increased risk of acute coronary events associated to vascular calcification, who may benefit from intensified preventative measures and for monitoring therapeutic efficacy is a major, ongoing challenge [46]. Recent publications have suggested that ECs directly contribute to vascular calcification through EndMT [2-4,42]. We have investigated the interplay between inflammatory cytokines and BMPs, a subfamily of the TGF-β family, in ECs. We found that the proinflammatory cytokine TNF-α induces EndMT in HAoECs, thereby enhancing their differentiation into osteoblast-like cells in response to BMP-9. TNF-α and IL-1β-induced EndMT in HAoECs, which results in BMPR2 down regulation. BMPR2 loss is sufficient and necessary for TNF-α to trigger EndMT in HAoECs. In addition, BMPR2 down regulation coincides with neointima formation and decrease of luminal PECAM1 positive cells in ApoE3Leiden mice subjected to high fat diet. Moreover, we showed that, in the absence of BMPR2, BMP-9 induces the formation of a receptor complex involving ACVR2A to induce downstream canonical signaling. Interestingly, we identified that BMPR2 down regulation leads to decreased JNK activation in ECs, as measured by phosphorylation of its downstream target c-JUN, and showed that JNK deactivation facilitates BMP-induced mineralization in ECs. Finally, we showed that adventitial microvessels (*vasa vasora*) in advanced atherosclerotic disease exhibit loss of luminal PECAM1 and BMPR2 expression and accumulation of PECAM1 αSMA double positive cells in layers underneath, which is suggestive of EndMT. Congruently, whereas p-SMAD1/5 activation increases in the *vasa vasora* ECs at early stages of atherosclerosis and remains sustained in advanced lesions, p-c-JUN activation dramatically drops in vessels in fibrotic calcified plaque lesions. These results point at a key role of BMPR2 as an integrator of TGF-β/BMP and inflammatory signaling in ECs, determining EndMT and subsequent calcification.

Endothelial cells with reduced BMPR2 expression displayed increased expression of inflammatory markers, such as ICAM and VCAM [47]. Interestingly, siRNA mediated knock-down of BMPR2 in human umbilical vein endothelial cells (HUVECs) led to reduced p-SMAD1/5 in response to BMP-4, although the authors did not test whether this effect was specific for BMPR2. BMP-9, unlike BMP-4, shows a high affinity for ALK1 in ECs [48] and BMPR2 [49], which may revert in a different contribution of BMPR2 in BMP-9 or BMP-4-induced receptor complexes. Furthermore, ALK1 (and not ALK2) was recently shown to mediate LDL uptake in ECs [50], and ECs exposed to an inflammatory cocktail lowered their LDL uptake capacity [51]. Whether BMPR2 deficiency alters the ALK1-LDL interaction is an interesting area of study.

BMPR2 deficiency leads to Pulmonary arterial hypertension (PAH), where heterozygous germ line mutations in the *BMPR2* gene are found in more than 70% of patients with hereditary PAH and 20% of patients with idiopathic PAH [52,53]. Several publications have pointed at EndMT as a causative factor for the vascular remodeling in the pulmonary arteries of PAH patients [54,55]. Furthermore, PAH patients display a higher tendency to develop calcified lesions within the pulmonary arteries [56], suggesting that BMPR2 may have a protective role inhibiting calcification in cells with osteogenic potential. In this sense, osteoblast specific knock out of *BMPR2* led to increased bone mass in transgenic mice [57]. Importantly, BMP-9 has been recently proposed as a therapeutic option for PAH [12]. Nevertheless, it remains to be determined whether systemic administration of BMP-9 may lead to calcification of the arteries under inflammatory conditions, such as those considered risk factors for atherosclerotic disease (renal disease, diabetes, hypertension or hyperlipidemia).

In summary, we have shown that aortic ECs undergo EndMT in response to inflammatory stimuli, which favour the calcification of ECs. The underlying mechanisms of such enhanced osteogenic potential point at non-canonical signal transduction, that fine tunes BMP-SMAD1/5 signaling (summarized in Figure S14). A hallmark of this process is the down regulation of BMPR2. Therefore, monitoring BMPR2 expression as a biomarker of calcification, or developing drugs specifically increasing BMPR2 expression to prevent EndMT in the arteries constitute an area of interest for future research.

Acknowledgements

We thank K. Iwata, S. Vukicevic and J. Nickel for reagents. We are grateful to Martijn Rabelink for shRNA lentiviral constructs. We thank Maarten van Dinther, Midory Thorikay, Kirsten Lodder and Karien Weismeijer for excellent technical assistance, and the entire group for scientific discussions. Research in the laboratory of PTD and MJG on TGF-β family is granted by the Netherlands Cardiovascular Research Initiative: the Dutch Heart Foundation, Dutch Federation of University Medical Centres, the Netherlands Organization for Health Research and Development, and the Royal Netherlands Academy of Sciences (PHAEDRA consortium) and by the gravitation program CancerGenomiCs.nl from the Netherlands Organization for Scientific Research (NWO). MJG and VP are supported by the BAV consortium (2013T093). GSD is supported by the RECONNECT consortium (belonging to the Netherlands Cardiovascular Research Initiative, as aforementioned) and a Postdoctoral Fellowship from AFM-Telethon. AGV would like to acknowledge the Dutch Arthritis Association (Reumafonds) for support.

Statement of author contributions

Study design: GSD, PtD, JL, MJG, MDV. *Data collection*: GSD, AGVA, VP, STGJ, MG. *Data analysis*: GSD, AGVA, VP, STGJ, MG. *Data interpretation*: GSD, PtD, JL, MJG, HVD, MDV. *Literature search*: GSD, PtD, JL, MJG, HVD, MDV. *Generation of figures*: GSD, AGVA, VP, STGJ. *Writing of the manuscript*: GSD, PtD, MJG, JL, HVD, MDV.

References

*Cited only in Supplementary Information.

1. Libby P, Ridker PM, Hansson GK. Progress and challenges in translating the biology of atherosclerosis. *Nature* 2011; **473**: 317–325.
2. Evrard SM, Lecce L, Michelis KC, *et al*. Endothelial to mesenchymal transition is common in atherosclerotic lesions and is associated with plaque instability. *Nat Commun* 2016; **7**: 1–15.
3. Sánchez-Duffhues G, de Vinuesa AG, Lindeman JH, *et al*. SLUG is expressed in endothelial cells lacking primary cilia to promote cellular calcification. *Arterioscler Thromb Vasc Biol* 2015; **35**: 616–627.
4. Chen P-Y, Qin L, Baeyens N, *et al*. Endothelial-to-mesenchymal transition drives atherosclerosis progression. *J Clin Invest* 2015; **125**: 4514–4528.
5. Sánchez-Duffhues G, García de Vinuesa A, ten Dijke P. Endothelial to mesenchymal transition in cardiovascular diseases: Developmental signalling pathways gone awry. *Dev Dyn* 2018; **247**: 492-508.
6. Gisterå A, Hansson GK. The immunology of atherosclerosis. *Nat Rev Neph* 2017; **13**: 368-380.
7. Boström K, Watson KE, Horn S, *et al*. Bone morphogenetic protein expression in human atherosclerotic lesions. *J Clin Invest* 1993; **91**: 1800–1809.
8. Dhore CR, Cleutjens JP, Lutgens E, *et al*. Differential expression of bone matrix regulatory proteins in human atherosclerotic plaques. *Arterioscler Thromb Vasc Biol* 2001; **21**: 1998–2003.
9. Morrell NW, Bloch DB, ten Dijke P, *et al*. Targeting BMP signalling in cardiovascular disease and anaemia. *Nat Rev Cardiol* 2016; **13**: 106–120.
10. David L, Mallet C, Keramidas M, *et al*. Bone morphogenetic protein-9 is a circulating vascular quiescence factor. *Circ Res* 2008; **102**: 914–922.
11. van Meeteren LA, Thorikay M, Bergqvist S, *et al*. Anti-human activin receptor-like kinase 1 (ALK1) antibody attenuates bone morphogenetic protein 9 (BMP9)-induced ALK1 signaling and interferes with endothelial cell sprouting. *J Biol Chem* 2012; **287**: 18551–18561.
12. Long L, Ormiston ML, Yang X, *et al*. Selective enhancement of endothelial BMPR-II with BMP9 reverses pulmonary arterial hypertension. *Nat Med*. 2015; **21**:777–785.
13. Mitrofan C-G, Appleby SL, Nash GB, *et al*. Bone morphogenetic protein 9 (BMP9) and BMP10 enhance tumor necrosis factor-α-induced monocyte recruitment to the vascular endothelium mainly via activin receptor-like kinase 2. *J Biol Chem* 2017; **292**: 13714–13726.

14. Kang Q, Sun MH, Cheng H, *et al.* Characterization of the distinct orthotopic bone-forming activity of 14 BMPs using recombinant adenovirus-mediated gene delivery. *Gene Ther* 2004; **11**: 1312–1320.
15. Saeed O, Otsuka F, Polavarapu R, *et al.* Pharmacological suppression of hepcidin increases macrophage cholesterol efflux and reduces foam cell formation and atherosclerosis. *Arterioscler Thromb Vasc Biol* 2012; **32**: 299–307.
16. Derwall M, Malhotra R, Lai CS, *et al.* Inhibition of bone morphogenetic protein signaling reduces vascular calcification and atherosclerosis. *Arterioscler Thromb Vasc Biol* 2012; **32**: 613–622.
17. de Vinuesa AG, Abdelilah-Seyfried S, Knaus P, *et al.* BMP signaling in vascular biology and dysfunction. *Cytokine Growth Factor Rev* 2016; **27**: 65–79.
18. de Jong DS, Vaes BLT, Dechering KJ, *et al.* Identification of novel regulators associated with early-phase osteoblast differentiation. *J Bone Miner Res* 2004; **19**: 947–958.
19. Zhang YE. Non-Smad pathways in TGF-β signaling. *Cell Res* 2009; **19**: 128–139.
20. Mu Y, Gudey SK, Landström M. Non-Smad signaling pathways. *Cell Tissue Res* 2012; **347**: 11–20.
21. Gilbert L, He X, Farmer P, *et al.* Inhibition of osteoblast differentiation by tumor necrosis factor-alpha. *Endocrinology* 2000; **141**: 3956–3964.
22. Kaneki H, Guo R, Chen D, *et al.* Tumor necrosis factor promotes Runx2 degradation through up-regulation of Smurf1 and Smurf2 in osteoblasts. *J Biol Chem* 2006; **281**: 4326–4333.
23. Gerstenfeld LC, Cho TJ, Kon T, *et al.* Impaired fracture healing in the absence of TNF-alpha signaling: the role of TNF-alpha in endochondral cartilage resorption. *J Bone Miner Res* 2003; **18**: 1584–1592.
24. Chang J, Wang Z, Tang E, *et al.* Inhibition of osteoblastic bone formation by nuclear factor-κB. *Nat Med* 2009; **15**: 682–689.
25. De Boeck M, Cui C, Mulder AA, *et al.* Smad6 determines BMP-regulated invasive behaviour of breast cancer cells in a zebrafish xenograft model. *Sci Rep* 2016; **6**: 24968.
26. Tasev D, van Wijhe MH, Weijers EM, *et al.* Long-Term Expansion in Platelet Lysate Increases Growth of Peripheral Blood-Derived Endothelial-Colony Forming Cells and Their Growth Factor-Induced Sprouting Capacity. *PLoS ONE* 2015; **10**: e0129935.
27. O'Connell KA, Rudmann AA. Cloned spindle and epithelioid cells from murine Kaposi's sarcoma-like tumors are of endothelial origin. *J Invest Dermatol* 1993; **100**: 742–745.
28. O'Connell K, Landman G, Farmer E, *et al.* Endothelial cells transformed by SV40 T antigen cause Kaposi's sarcomalike tumors in nude mice. *Am J Pathol* 1991; **139**: 743–749.
29. Zhang J, Zhang X, Zhang L, *et al.* LRP8 mediates Wnt/β-catenin signaling and controls osteoblast differentiation. *J Bone Miner Res* 2012; **27**: 2065–2074.

30. van Dinther M, Visser N, de Gorter DJJ, *et al*. ALK2 R206H mutation linked to fibrodysplasia ossificans progressiva confers constitutive activity to the BMP type I receptor and sensitizes mesenchymal cells to BMP-induced osteoblast differentiation and bone formation. *J Bone Miner Res* 2010; **25**: 1208–1215.
31. Hamdi M, Kool J, Cornelissen-Steijger P, *et al*. DNA damage in transcribed genes induces apoptosis via the JNK pathway and the JNK-phosphatase MKP-1. *Oncogene* 2005; **24**: 7135–7144.
32. Lardenoye JHP, de Vries MR, Löwik CWGM, *et al*. Accelerated atherosclerosis and calcification in vein grafts: a study in APOE*3 Leiden transgenic mice. *Circ Res* 2002; **91**: 577–584.
33. Virmani R, Kolodgie FD, Burke AP, *et al*. Lessons from sudden coronary death: a comprehensive morphological classification scheme for atherosclerotic lesions. *Arterioscler Thromb Vasc Biol* 2000; **20**: 1262–1275.
34. van Dijk RA, Virmani R, Thüsen von der JH, *et al*. The natural history of aortic atherosclerosis: a systematic histopathological evaluation of the peri-renal region. *Atherosclerosis* 2010; **210**: 100–106.
35. Korchynskyi O, ten Dijke P. Identification and functional characterization of distinct critically important bone morphogenetic protein-specific response elements in the Id1 promoter. *J Biol Chem* 2002; **277**: 4883–4891.
36. Rennefahrt UEE, Illert B, Kerkhoff E, *et al*. Constitutive JNK activation in NIH 3T3 fibroblasts induces a partially transformed phenotype. *J Biol Chem* 2002; **277**: 29510–29518.
37. Scharpfenecker M, van Dinther M, Liu Z, *et al*. BMP-9 signals via ALK1 and inhibits bFGF-induced endothelial cell proliferation and VEGF-stimulated angiogenesis. *J Cell Sci* 2007; **120**: 964–972.
38. Rosenzweig BL, Imamura T, Okadome T, *et al*. Cloning and characterization of a human type II receptor for bone morphogenetic proteins. *Proc Natl Acad Sci USA* 1995; **92**: 7632–7636.
39. Ichijo H, Yamashita H, ten Dijke P, *et al*. Characterization of in vivo phosphorylation of activin type II receptor. *Biochem Biophys Res Commun* 1993; **194**: 1508–1514.
40. ten Dijke P, Yamashita H, Ichijo H, *et al*. Characterization of type I receptors for transforming growth factor-b and activin. *Science* 1994; **264**: 101–104.
41. Upton PD, Morrell NW. TGF-β and BMPR-II pharmacology--implications for pulmonary vascular diseases. *Curr Opin Pharmacol* 2009; **9**: 274–280.
42. Guihard PJ, Yao J, Blazquez-Medela AM, *et al*. Endothelial-Mesenchymal Transition in Vascular Calcification of Ins2Akita/+ Mice. Ushio-Fukai M, editor. *PLoS ONE* 2016; **11**: e0167936–12.
43. Wang L, Luo J-Y, Li B, *et al*. Integrin-YAP/TAZ-JNK cascade mediates atheroprotective effect of unidirectional shear flow. *Nature* 2016; **540**: 579–582.

44. Podkowa M, Zhao X, Chow C-W, *et al.* Microtubule stabilization by bone morphogenetic protein receptor-mediated scaffolding of c-Jun N-terminal kinase promotes dendrite formation. *Mol Cell Biol* 2010; **30**: 2241–2250.
45. Chen W-K, Yeap YYC, Bogoyevitch MA. The JNK1/JNK3 interactome--contributions by the JNK3 unique N-terminus and JNK common docking site residues. *Biochem Biophys Res Commun* 2014; **453**: 576–581.
46. Franco M, Cooper RS, Bilal U, *et al.* Challenges and Opportunities for Cardiovascular Disease Prevention. *Am J Med* 2011; **124**: 95–102.
47. Kim CW, Song H, Kumar S, *et al.* Anti-inflammatory and antiatherogenic role of BMP receptor II in endothelial cells. *Arterioscler Thromb Vasc Biol* 2013; **33**: 1350–1359.
48. Scharpfenecker M, van Dinther M, Liu Z, *et al.* BMP-9 signals via ALK1 and inhibits bFGF-induced endothelial cell proliferation and VEGF-stimulated angiogenesis. *J Cell Sci* 2007; **120**: 964–972.
49. Kraehling JR, Chidlow JH, Rajagopal C, *et al.* Genome-wide RNAi screen reveals ALK1 mediates LDL uptake and transcytosis in endothelial cells. *Nature Commun* 2016; **7**: 1–15.
50. Rieder F, Kessler SP, West GA, *et al.* Inflammation-induced endothelial-to-mesenchymal transition: a novel mechanism of intestinal fibrosis. *Am J Pathol* 2011; **179**: 2660–2673.
51. Brown MA, Zhao Q, Baker KA, *et al.* Crystal structure of BMP-9 and functional interactions with pro-region and receptors. *J Biol Chem* 2005; **280**: 25111–25118.
52. International PPH Consortium, Lane KB, Machado RD, *et al.* Heterozygous germline mutations in BMPR2, encoding a TGF-β receptor, cause familial primary pulmonary hypertension. *Nat Genet* 2000; **26**: 81–84.
53. Deng Z, Morse JH, Slager SL, *et al.* Familial primary pulmonary hypertension (gene PPH1) is caused by mutations in the bone morphogenetic protein receptor-II gene. *Am J Hum Genet* 2000; **67**: 737–744.
54. Ranchoux B, Antigny F, Rucker-Martin C, *et al.* Endothelial-to-Mesenchymal Transition in Pulmonary Hypertension. *Circulation* 2015; **131**: 1006-1018.
55. Qiao L, Nishimura T, Shi L, *et al.* Endothelial fate mapping in mice with pulmonary hypertension. *Circulation* 2014; **129**: 692–703.
56. Ruffenach G, Chabot S, Tanguay VF, *et al.* Role for Runt-related Transcription Factor 2 in Proliferative and Calcified Vascular Lesions in Pulmonary Arterial Hypertension. *Am J Respir Crit Care Med* 2016; **194**: 1273–1285.
57. Lowery JW, Intini G, Gamer L, *et al.* Loss of BMPR2 leads to high bone mass due to increased osteoblast activity. *J Cell Sci* 2015; **128**: 1308–1315.
*58. Nakao A, Imamura T, Souchelnytskyi S, *et al.* TGF-β receptor-mediated signalling through Smad2, Smad3 and Smad4. *EMBO J* 1997; **16**: 5353–5362.

*59. Zou Y, Dietrich H, Hu Y, *et al*. Mouse model of venous bypass graft arteriosclerosis. *Am J Pathol* 1998; **153**: 1301–1310.

*60. Hawinkels LJAC, Paauwe M, Verspaget HW, *et al*. Interaction with colon cancer cells hyperactivates TGF-β signaling in cancer-associated fibroblasts. *Oncogene* 2014; **33**: 97–107.

Supplemental figures

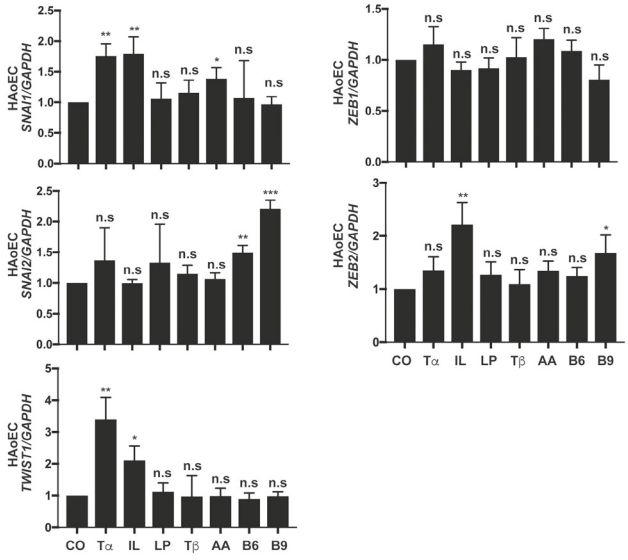

Figure S1. TNF-α and IL-1β induce the up-regulation of EndMT factors in HAoECs. Gene expression analysis of the genes SNAI1 (encoding SNAIL), SNAI2 (encoding SLUG), TWIST1, ZEB1 and ZEB2 in HAoECs stimulated for 24 h with the indicated cytokines and growth factors. CO: control; Tα: TNF-α (10 ng/ml); IL: IL-1β (10 ng/ml); LP: LPS (10 ng/ml); Tβ: TGF-β3 (5 ng/ml); AA: activin A (50 ng/ml); B6: BMP-6 (50 ng/ml); B9: BMP-9 (10 ng/ml).

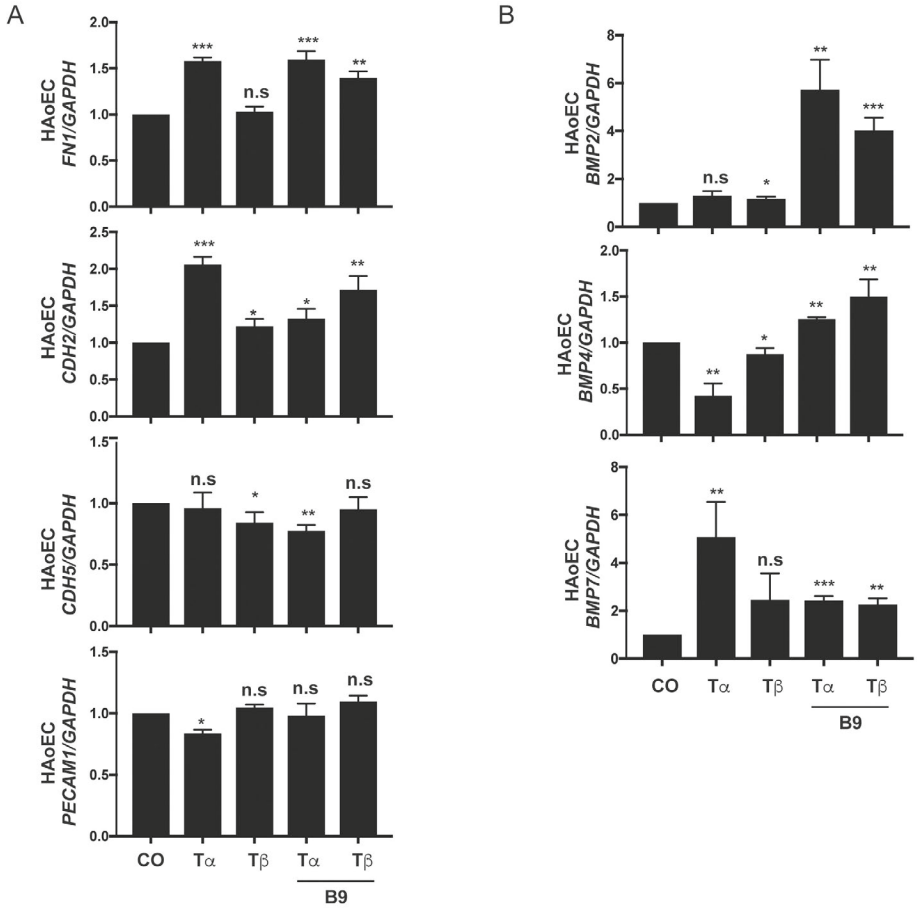

Figure S2. Long term effect of TNF-α and TGF-β in HAoECs. A. Gene expression analysis of FN (encoding Fibronectin), CDH2 (encoding N-CAHDERIN), CDH5 (encoding VE-CADHERIN) and PECAM1 in HAoECs stimulated for 4 days with TNF-α (Tα: 10 ng/ml) or TGF-β3 (Tβ: 5 ng/ml); followed by 24 h of BMP-9 (B9: 10 ng/ml). B. qPCR gene expression analysis of the BMP ligand encoding genes BMP2, BMP4 and BMP7, in HAoECs treated as indicated in (A).

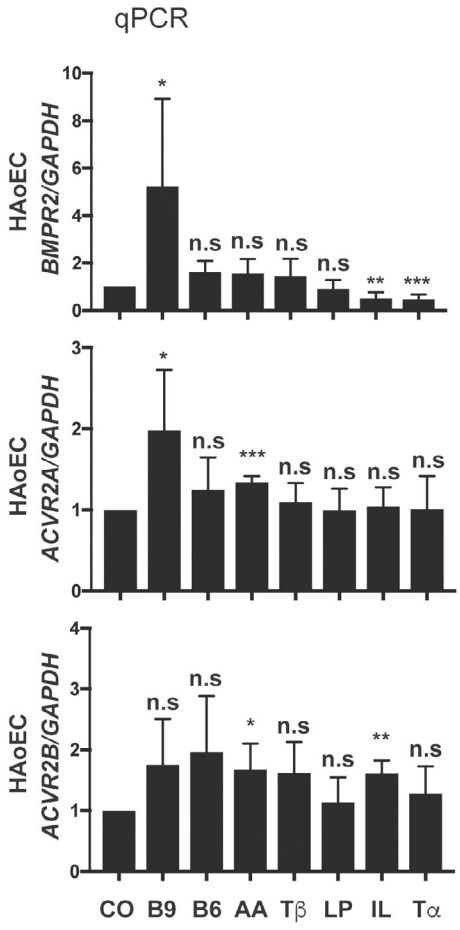

Figure S3. TNF-α and IL-1β induce the down regulation of BMPR2 in HAoECs. Gene expression analysis of the BMP type II receptors BMPR2, ACVR2A and ACVR2B in HAoECs incubated for 24 h with the indicated growth factors in the presence of 10% of serum.

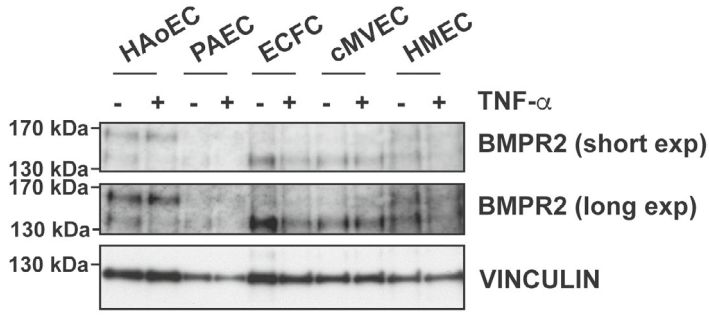

Figure S4: TNF-α induces the up-regulation of BMPR2 in a cell type specific manner. Western blot for BMPR2 (long and short exposures) in HAoEC, human pulmonary aortic ECs (PAEC), human endothelial colony forming cells (ECFC), human coronary microvascular EC (cMVEC) and human skin microvascular ECs (HMEC) treated for 24 h with TNF-α (10 ng/ml) in medium containing 10% serum.

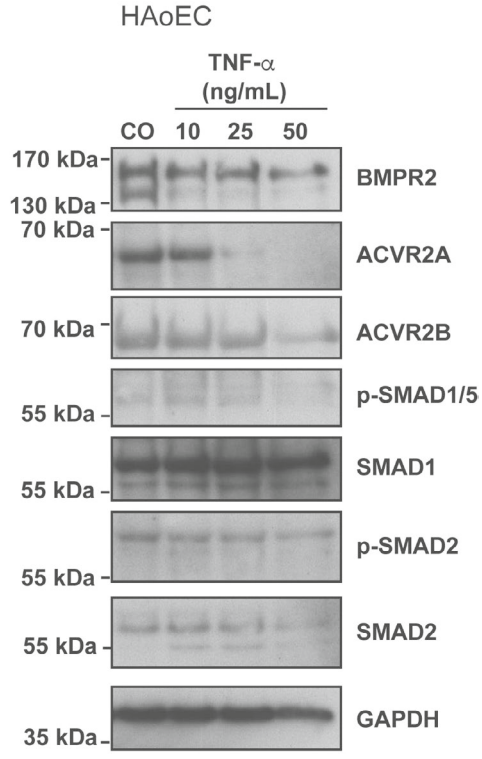

Figure S5. TNF-α down regulates BMPR2 in a dose dependent manner. Western blot in HAoECs treated for 24 h with increasing concentrations of TNF-α in medium containing 10% serum. CO: Control.

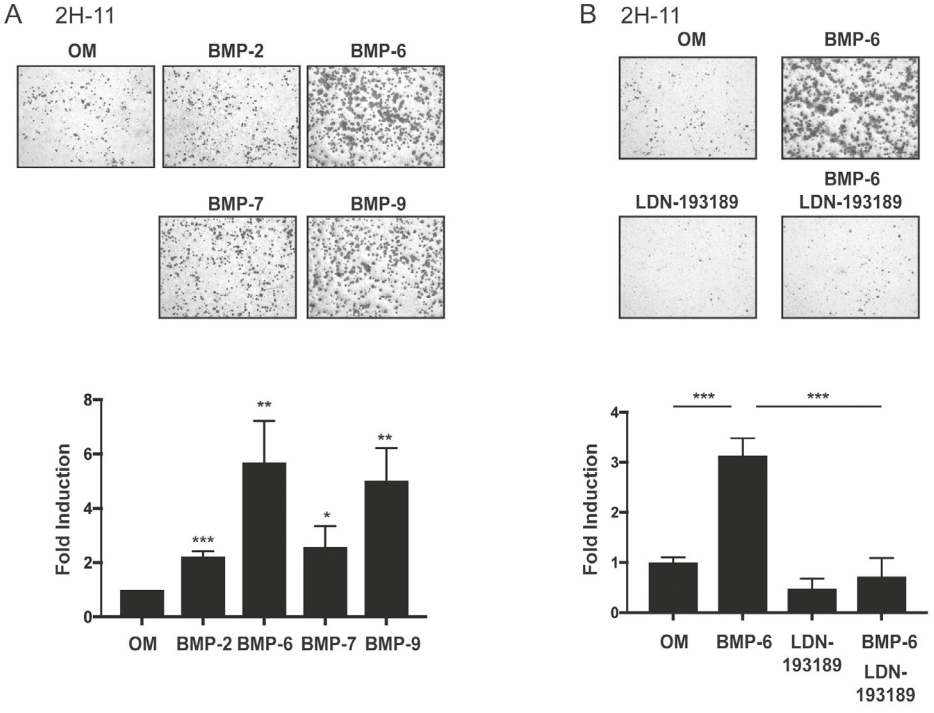

Figure S6. BMP receptor activation is required to induce cell mineralization in 2H-11 endothelial cells. A. Alizarin Red staining (ARS) of 2H-11 cells stimulated with either BMP-2, BMP-6 or BMP-7 (50 ng/ml) or BMP-9 (10 ng/ml) for 14 days under osteogenic culture conditions (OM). Quantification is shown below as fold induction of OM control cells. B. ARS of 2H-11 cells stimulated for 14 days with BMP-6 (50 ng/ml) and/or the BMP type I receptor kinase inhibitor LDN-193189 (120 nM). Quantification is shown below as fold induction of OM control cells.

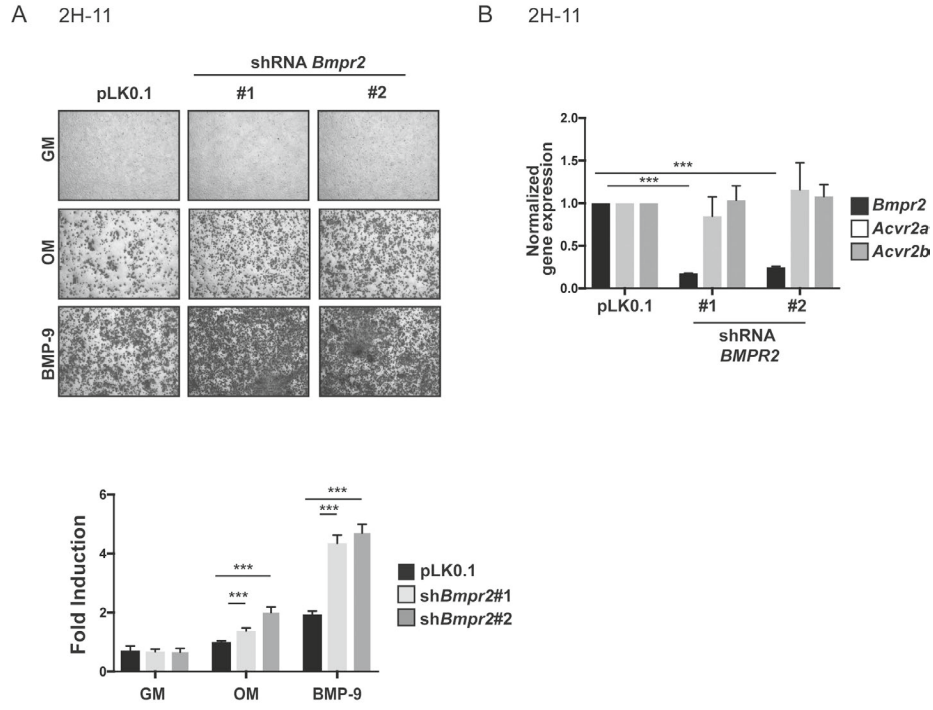

Figure S7. BMPR2 knock-down enhances BMP-9 induced mineralization in 2H-11 cells. A. Alizarin Red staining (ARS) of 2H-11 cells stably transduced with two independent shRNA constructs targeting BMPR2 (#1 and #2) or an empty vector (pLK0.1) and incubated with BMP-9 (10 ng/ml) for 14 days under osteogenic culture conditions (OM) or regular growth medium (GM). Quantification is shown below as fold induction of pLK0.1 stable cells in OM. B. qPCR analysis of BMPR2, ACVR2A and ACVR2B in 2H-11 cells knocked down for BMPR2.

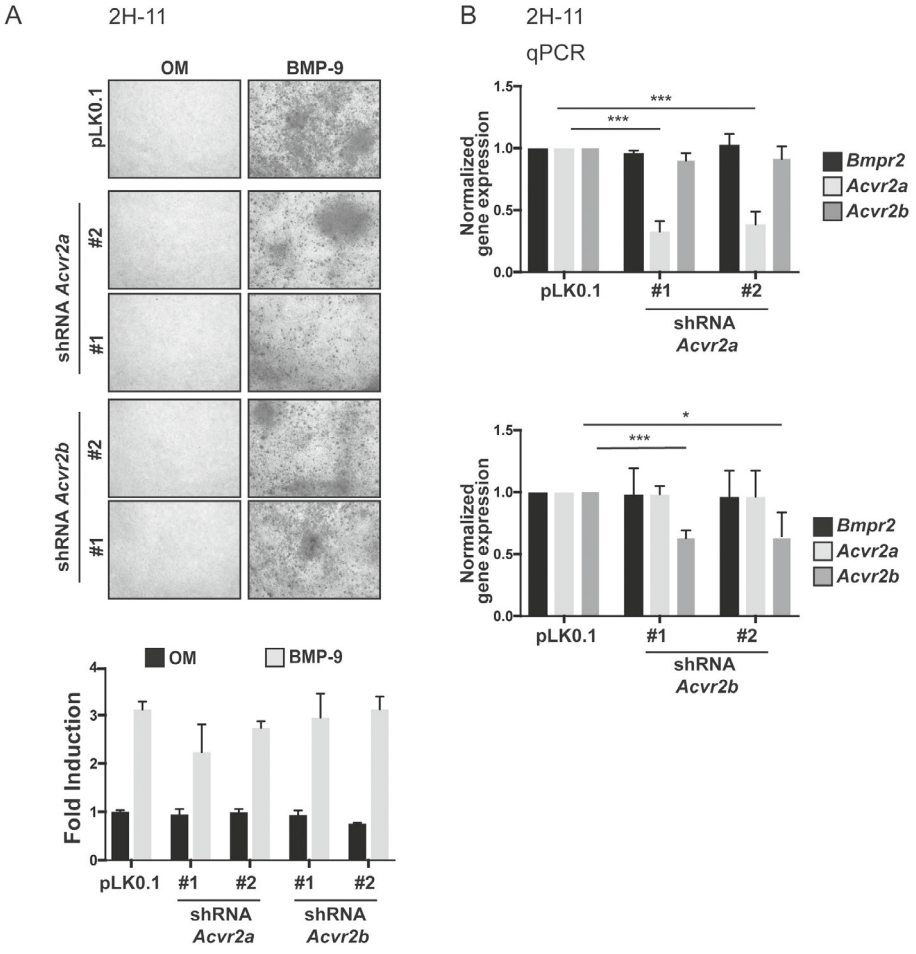

Figure S8. Knock-down of ACVR2A or ACVR2B does not affect BMP-9 induced mineralization in 2H-11 cells. A. ARS of 2H-11 cells stably transduced with two shRNA constructs targeting Acvr2A or Acvr2B (#1 and #2) or a control vector (pLK0.1) and incubated with BMP-9 (10 ng/ml) for 14 days under osteogenic culture conditions (OM) or regular growth medium (GM). Quantification is shown below as fold induction of pLK0.1 stable cells in OM. B. qPCR analysis of Bmpr2, Acvr2A and Acv2 in 2H-11 cells knocked down for AcvrA and Acvr2B.

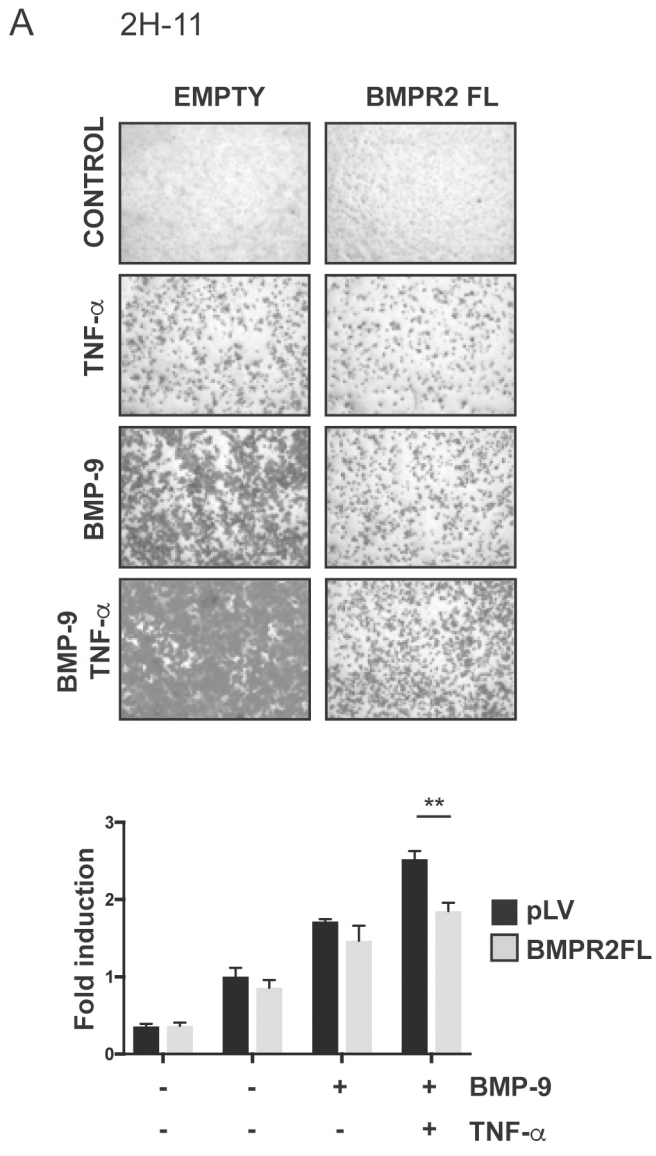

Figure S9. BMPR2 over-expression partially prevents BMP-9 induced mineralization in 2H-11 cells. ARS of 2H-11 cells stably over-expressing a BMPR2 full length construct (BMPR2 FL) or an empty vector (EMPTY, pLV) and stimulated with BMP-9 (10 ng/ml) and/or TNF-α (10 ng/ml) for 14 days under osteogenic conditions. Quantification is shown below as fold induction of pLV stable cells in OM.

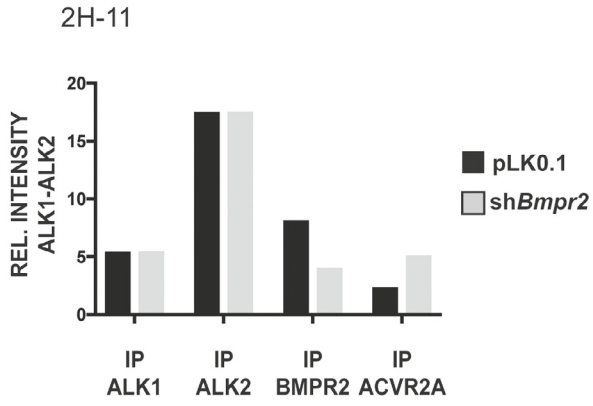

Figure S10. Knock-down of BMPR2 does not compromise BMP-9 binding to ALK1 or ALK2. Quantification by densitometry corresponding to a ligand-receptor interaction assay performed in 2H-11 stably infected with a control (pLK0.1) or BMPR2 knock-down (shBMPR2) lentivirus. ALK1-ALK2 intensity is shown. IP: Immunoprecipitation.

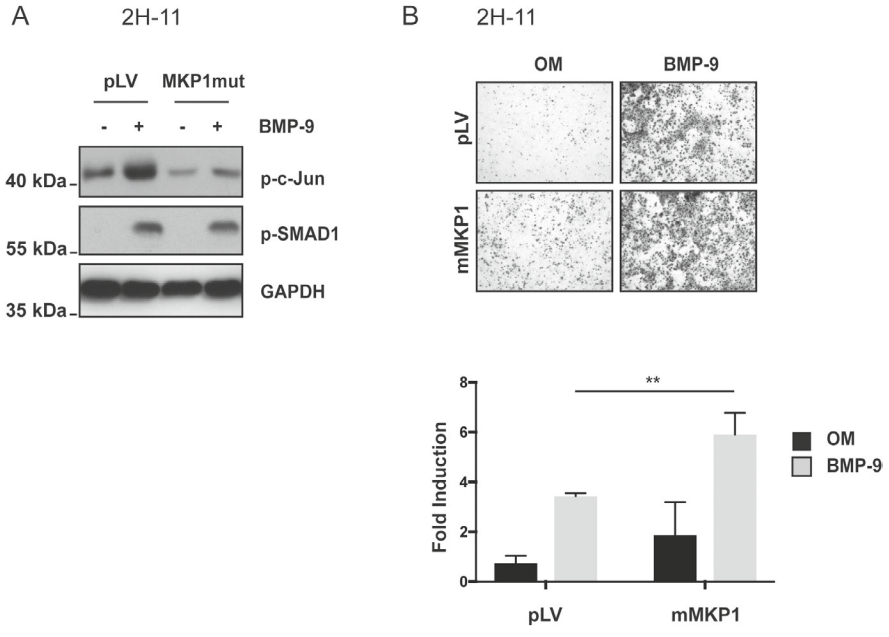

Figure S11. Inhibition of c-Jun phosphorylation enhances BMP-9 induced mineralization in 2H-11 cells. A. Western blot of 2H-11 cells transduced with lentivirus encoding for a c-Jun-specific mutant version of MKP1 (mMKP1) or an empty vector and stimulated with BMP-9 (10 ng/ml). B. ARS of 2H-11 cells infected with mMKP1 and stimulated with BMP-9 (10 ng/ml) under osteogenic culture conditions (OM). Calcium deposits were solubilized and measured by absorbance.

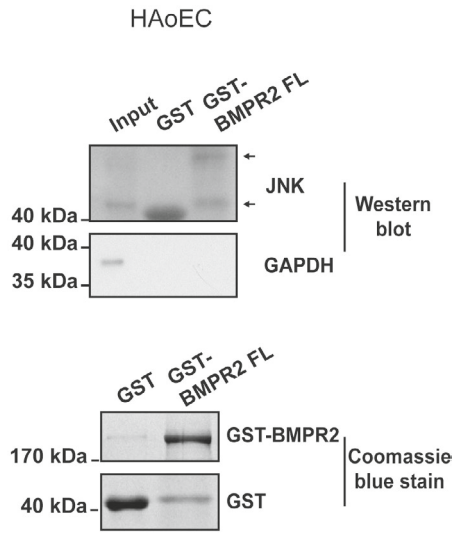

Figure S12. *In vitro* protein interaction BMPR2-JNK. JNK interacts with BMPR2 in GST-BMPR2 pull down assay on whole cell lysate of HAoECs. Endogenous JNK interacts *in vitro* with GST-BMPR2 FL, whereas GAPDH is only detected in the input.

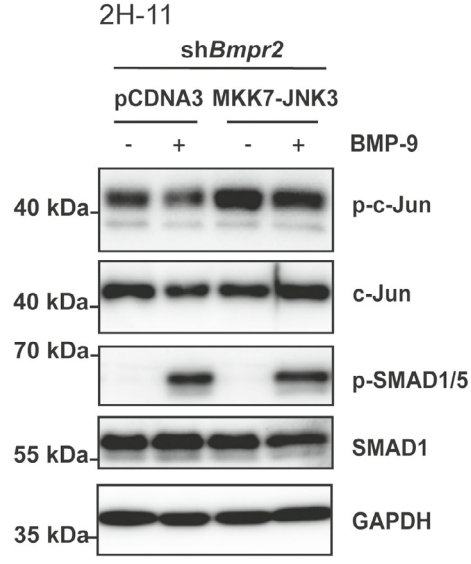

Figure S13. MKK7-JNK3 over expression restores p-c-Jun in 2H-11 shBMPR2 cells. Western blot of 2H-11 cells stably knocked-down for BMPR2 and transfected with a MKK7-JNK3 encoding construct or an empty vector (pcDNA3). Cells were serum starved for 16 h and stimulated for 45 min with BMP-9 (10 ng/ml).

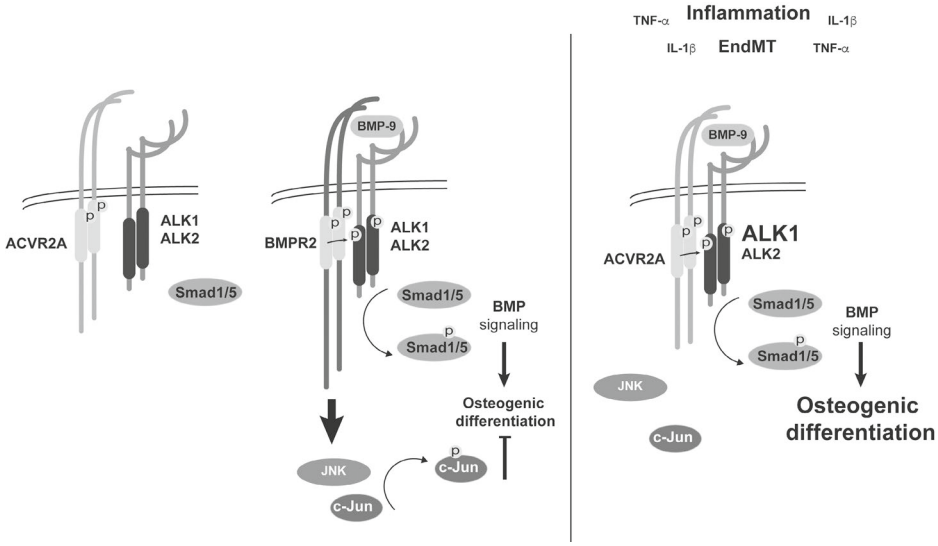

Figure S14. Graphical summary. In the presence of BMP-9, a heterotetrameric BMP membrane receptor complex is formed consisting of ALK1/2 and BMPR2 in ECs. This induces the downstream activation of canonical SMAD1/5 and non-canonical JNK signaling, leading to osteogenic differentiation and calcium deposition. Upon stimulation with TNF-α, ECs undergo EndMT and down-regulate BMPR2. BMP-9 now interacts with a receptor complex consisting of ALK1/2 and ACVR2A in ECs. This induces the phosphorylation of SMAD1/5, but does not activate p-c-Jun potently. As p-c-Jun acts as a negative regulator of EC calcification, EndMT-derived cells exhibit a higher osteogenic activity in response to BMP-9.